CrossMark

Formation mechanism and kinetic analysis of the morphology of Cu_6Sn_5 in the spherical solder joints at the Sn/Cu liquid–solid interface during soldering cooling stage

Bingfeng Guo[1] · Haitao Ma[1] · Chengrong Jiang[1] · Yunpeng Wang[1] · Anil Kunwar[1] · Ning Zhao[1] · Mingliang Huang[1]

Abstract The morphology evolution mechanism and dynamics of Cu_6Sn_5 intermetallic compound (IMC) in cooling stage were studied by using pure Sn solder ball with a diameter of 1 mm to react with polycrystalline Cu substrate and form Cu_6Sn_5. A nearly uniform height of the scallop-like IMC grains is attained by using high pressurized air to remove excess liquid solder (that is, for acquisition of the IMC morphology identical to heat preservation stage). But the morphology evolution of IMC in the solder joint was greatly affected by the cooling phase of interfacial reaction, and IMC morphology partition phenomenon was found in the spherical joints. The IMC at the edge portion characterized scallop morphology whereas the central portion possessed prismatic shape morphology. Finite element simulation for the temperature field distribution in the solder ball-substrate domain showed temperature gradient in solder's internal core was significantly greater than that at the edge. Using this simulation results with kinetic equations, it could be understood that the central core region is conducive to the formation of small plane structure morphology. These small planes would eventually form the prismatic morphology IMC in the central region. As the soldering temperature increases, the area ratio of IMC with scallop-like morphology to the prismatic shaped IMC reduced from 0.2178 down to 0.1680. Moreover, for an elevated temperature of 300 °C, it is observed that the central region IMC (with prismatic structure) grows upto an average thickness of 7.7245 μm, whereas the thickness value for scalloped IMC at the edge portion is around 4.556 μm.

✉ Haitao Ma
htma@dlut.edu.cn

[1] School of Materials Science and Engineering, Dalian University of Technology, Dalian 116024, China

1 Introduction

With the awareness of the environmental problem and human health, people have advocated for the prohibition of the usage of Pb-containing solder [1]. Thus lead-free solders have attracted attention in microelectronics interconnect industries. The microstructure of solder joint has great influence on the reliability of electronic packaging interconnection, and the microstructure of solder joint is affected by the reaction and diffusion during brazing process and service process. Numerous studies have showed that the intermetallic compound (IMC) of welded joints is an important factor affecting the reliability of the joint [2–4]. Due to the intrinsic brittleness of the IMC, the interfacial IMC layer type, thickness, morphology and distribution of elements significantly affect lead-free solder interconnect reliability [5, 6], so the morphology of a solder joint and distribution of heterogeneity of the IMC, will inevitably affect the reliability of solder joints and packaging. Yang et al. [7] have studied the morphology of Cu_6Sn_5 in Sn–Ag/Cu brazed joint by using a scanning electron microscope, in which the reaction time is 60 s and under different soldering temperature. It was found that the morphology of Cu_6Sn_5 changed from scallop shape to small flat shape with the increasing of temperature, growing up to a long prismatic eventually. In addition to this, it was also found that the shear strength was associated with IMC morphology and thickness. Prismatic grain has a strong inhibition effect on dislocation motion and crack propagation. The crack has more difficulties to split protruding prismatic grains than to extend on the scallop-shaped grains, when the crack needed to extend. Thus, the prismatic grains joints have greater shear strength than scallop grains. As the brazing temperature is increased, IMC thickness increases and the shear strength continues to decline. Meanwhile, Lee et al. [8], who studied

the Sn–Ag/Cu soldering joint relationship between the tensile strength and the morphology and thickness of IMC, also found that the tensile strength declined with the roughness and thickness of IMC increased, and studied the stress distribution of Sn–Ag/Cu brazing joint by using FEM simulation found that stress centralization in the solder/Cu_6Sn_5 interface was easy to induce the formation and growth of crack. The cracks appeared in the solder/Cu_6Sn_5 interface and propagated along the interface when the IMC thickness was less than 1 μm while the thickness of IMC was 1–10 μm, cracks appeared near the prominent Cu_6Sn_5 waist then toward with the solder/Cu_6Sn_5 interface with the direction of approximately 45° extending into the solder, ultimately forms dimple fracture morphology. When the IMC thickness exceeded 10 μm, solder/Cu interface became rough and was accompanied with the residual stress which caused by the transformation of the crack produced and extended in the Cu_6Sn_5 layer. Therefore, it is necessary to study the formation mechanism of the solder joint of IMC morphology and distribution of non-uniform. However, most of researchers only studied the influence of the sample's morphology in the complete brazing cooling progress on the mechanical properties of welded joints, with only a few studies on the formation mechanism of IMC morphology and distribution in the solder joints. As there is only a limited availability of conventional experimental means at present, to distinguish the results of cooling stage of soldering; the volume of research works regarding IMC morphology, distribution and formation mechanism in single solder joint is currently not quite so large.

In this paper, the experimental method of using high pressure air to remove the liquid solder is presented to obtain exact morphology of IMC during the heat preservation stage. By comparing complete air cooling samples under the same condition of soldering, we have obtained the cooling stage of soldering from complete air cooling. Therefore, the thickness, morphology and distribution of the IMC of solder joints cooling stage are studied explicitly. In addition, the growth rates of IMC on Sn/Cu liquid–solid interface is directly observed by using synchrotron radiation real-time dynamic imaging technology in Shanghai

light source. Then, the formation mechanism and dynamics of the IMC morphology and distribution in solder cooling stage is analyzed by using the finite element to simulate the temperature field inside the solder joint. And the effect of temperature on the morphology and thickness of IMC in soldering stage was also studied.

2 Experiment details

The pure Sn (99.99%) solder with a diameter of 1 mm solder ball is used to react with polycrystalline Cu (99.99%, the size: 2000 μm × 2000 μm × 100 μm) substrate in the reflow furnace at 250, 275, 300 °C with reaction time being 5 min. Then, the sample is allowed to undergo either cooling in air (7.4 °C/s) as shown in Fig. 1a and or retain IMC morphology of reflow heating stage via utilization of high-pressure air (0.8 Mpa) to remove excess liquid solder (that is, for acquisition of the IMC morphology at heat preservation stage) as shown in Fig. 1b. Heat preservation stage is the phase in this experiment in which the reflow soldering temperature is held constant for 5 min. This stage lies in between the heating and cooling stage. Two kinds of cooling samples are prepared for SEM by grinding, polishing, etching with 5% HNO_3 + 2% HCl + 93% C_2H_5OH (in volume) solution to reveal the cross-sectional morphology. Similarly, some samples were etched by 10% HNO_3 solution (in volume) to remove the solder away for top-view observation. The top-view and cross-sectional-view of IMC are observed by SEM. In addition, the growth of IMC at Sn/Cu liquid–solid interface under 350 °C is directly observed by synchrotron radiation real-time dynamic imaging technology in Shanghai light source BL13W1 line station. The thickness of the solders (pure Sn) and Cu substrate were all 100 μm. The cross-section of the Cu substrate was polished and a butt joint was made to connect it with the solder, having lead-free flux (AMTECH: NC-559-ASM) in between. Schematic diagrams of synchrotron radiation as shown in Fig. 1c. Two pieces of Al_2O_3 ceramics with a thickness of 280 μm were used to seal the Cu substrate and solder together. The energy of the monochromatic beam was
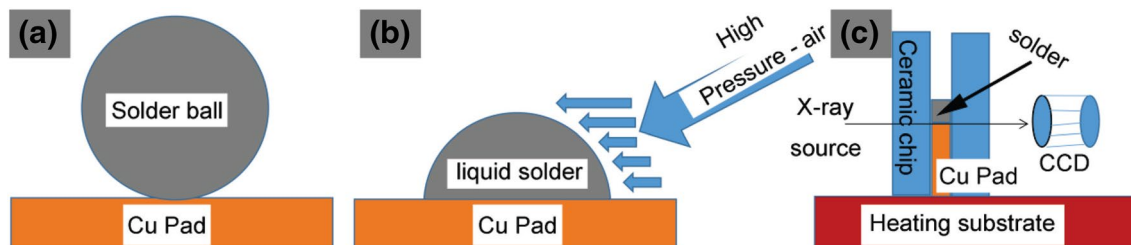
Fig. 1 Schematic diagrams of reflow soldering sample (**a**), liquid solder removed by liquid solder (**b**) and configuration for synchrotron radiation experiment (**c**)

28 keV and a charge coupled device with resolution ratios of 0.37 and 0.325 μm/pix was used, and the corresponding exposure time was 5 and 0.5 s, respectively. The samples were put into a specially designed soldering furnace with a hole through which the formation and evolution of interfacial bubbles during the soldering process could be observed by the synchrotron radiation real-time imaging technology. The specimen preparation was similar to that in the previous study [9, 10].

3 Result and discussion

3.1 Correlating the degree of supercooling and IMC morphology

On the micro scale, the surface of a crystal can be divided into rough interface and smooth interface in accordance to the roughness criteria [11]. The smooth interface of the crystal has a tendency to form a small plane structure. Rough interface, on the other hand tends to form a smooth surface with the curvature. On the basis of experimental observation of the actual growth morphology of interfacial IMC, the small plane structure corresponds to the smooth interface [11–13]. The IMC region of formation of small plane is the boundary between predominantly scalloped IMC and prismatic morphology. The shape of the hemispherical and scallop shaped surface is corresponding to the rough interface, and is mainly controlled by the continuous growth mechanism [11–13]. The growth difference between the rough interface and the smooth surface depends on the required degree of the supercooling of different growth mechanism. Generally, the required degree of supercooling of the small plane growth is larger with the same crystal growth rate. In the same degree of supercooling, the growth rate of the small planar structure is the slowest [12]. At the same time, the crystals formed under the control of different growth mechanisms still follow their inherent dynamic mechanism during the growth process.

Different growth mechanisms corresponding to the crystal growth rate G can be expressed as follows [11]:

$$G = A \exp\left(-\frac{B}{\Delta T}\right) \quad \text{Two dimensional nucleation mechanism}$$
(1)

$$G = A\Delta T \quad \text{Continuous growth mechanism}$$
(2)

where A is IMC growth kinetics coefficient, B is the Boltzmann constant, ΔT is the degree of cooling, G is growth rate of IMC. It can be seen from the expression that for the same degree of supercooling the performance of the IMC growth rates vary greatly [13]. If the crystals are grown at the same rate as the G under different growth mechanisms,

the degree of cooling in different growth mechanisms is as follows:

$$\Delta T_0 = \frac{-B_0}{\ln(G/A_0)} \quad \text{Two dimensional nucleation mechanism}$$
(3)

$$\Delta T_1 = G/A_1 \quad \text{Continuous growth mechanism}$$
(4)

wherein A_0, A_1 is the IMC growth kinetics coefficient, ΔT_0, ΔT_1 is the degree of cooling, G is the growth rate of IMC. Typically, in the same growth rate G, the required degree of cooling of the two mechanisms is:

$$\Delta T_0 > \Delta T_1$$
(5)

The relative degree of cooling can be expressed as delta $T = \Delta T_0 - \Delta T_1$. From the Eq. (5), it can be inferred that $\Delta T > 0$. This shows that the required degree of cooling of scallop shaped grain is smaller than a small planar structure at the same growth rate in the same sample, and the position of the small plane should be in a relatively low temperature region.

The expression of a small plane can be expressed as:

$$S \approx 2\Delta Tr/W$$
(6)

where S is the area of the small plane, ΔT is relative degree of supercooling of a small plane center with respect to the hemispherical, r is the radius of curvature of the IMC, W is the liquid/solid interface temperature gradient. In Eq. (5), since ΔT is greater than 0; IMC is the outer convex shape from the solid phase into the liquid solder at the solder interface, so the radius of curvature r here is greater than 0. Then the necessary condition for the formation of a small plane at the interface can only depend on the positive and negative of W. Small plane is formed when the W and S are positive, while it is suppressed when the these parameters are negative.

3.2 IMC morphology of spherical solder joints in the heat preservation stage and complete air cooling

Figure 2 is the SEM image for IMC morphology at 275 °C, formed after soldering reaction of Sn with the polycrystalline Cu substrate and subsequently being subjected either to solder removal via highly pressurized air or to normal air cooling with the time period of 5 min.

High-pressure air removing excess liquid solder is equivalent to the soldering process without cooling stage, which is the soldering heat preservation stage. In heat preservation stage, the solder ball spreading area is totally flat (Fig. 2a). The top-view morphology of IMC observed from the magnification this area as shown in Fig. 2b, can be characterized to be mostly scalloped with few small plane structure
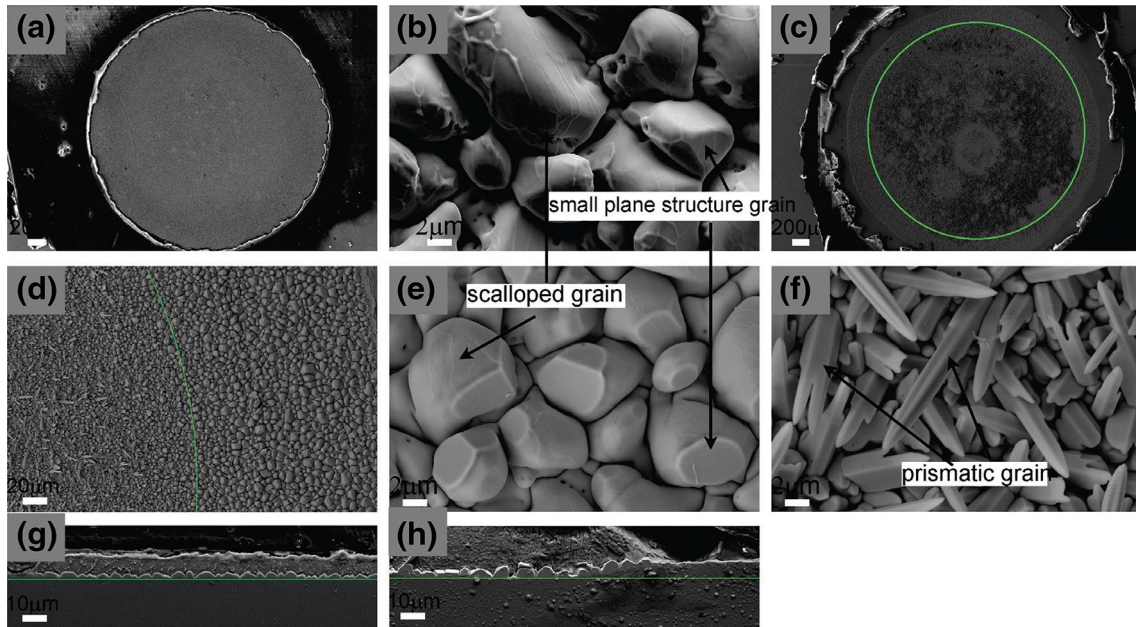
Fig. 2 SEM image of the *top-view* (**a**–**f**) and cross-sectional (**g, h**) morphologies of IMC grains in samples treated with high-pressure air and air cooling under 275 °C at 5 min. Solder ball spreading area under high-pressure air (**a**) and air cooling (**c**)

grains. The cross-section view presented in Fig. 2g exhibit a nearly uniform height of the IMC grains. This phenomenon is consistent with findings of Qu et al. [10]. As compared to the morphology of heat preservation stage, it is found for air cooling condition that the morphology of IMC varies along the area of a solder joint. Figure 2d is the magnified image of a portion of the solder ball of Fig. 2c having undergone air cooling. As shown in the figure, scalloped grains appearance is more noticeable at the edge of spreading area of solder ball whereas the central part of the IMC morphology is irregular. These regions are demarcated by a green colored arc. For greater magnifications

of the regions of the edge and central portions, it has been learnt that IMC corresponding to the edge region (Fig. 2e) are characterized with scalloped plus faceted morphology whereas the IMC for central portion (Fig. 2f) exhibit prismatic morphology. Moreover in the cross-sectional image for this air-cooled solder (Fig. 2h), it can also be observed that the edge part is scalloped and the central part of IMC morphology is prismatic.

Figure 3 shows synchrotron radiation image of Sn/Cu joint being soldered at 250/275/300/350 °C. The gray zone in top is liquid Sn, the black zone at the bottom is Cu substrate, and the intermediate colored zone between Sn and

Fig. 3 Synchrotron radiation images of a Sn/Cu joint during soldering at 250/275/300/350 °C. **a** 0 min is initial stage, **b** 0 to 60 min is heat preservation stage
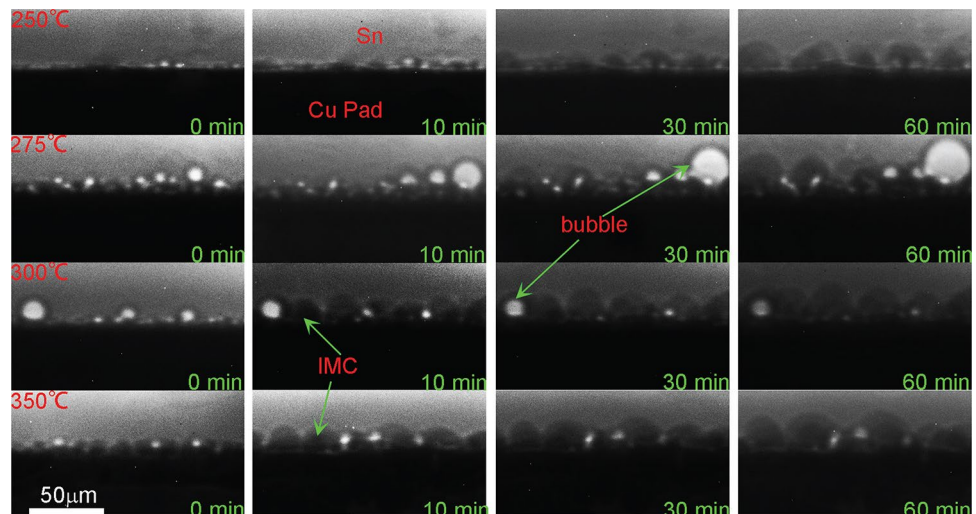
Cu consisted of IMC grain. In the figures, the white colored bubbles are also shown along the interface. As shown in Fig. 3, the morphology of IMC is scallop-like shape when the soldering time reached 10 min. However, IMC is still scallop-like when the soldering time extends to 60 min. Thus, this result is consistent with the result of heat preservation stage as shown in Fig. 2g.

From the combined results of SEM images and synchrotron radiation experiments, it can be inferred that the IMC morphology in the heat preservation stage is scallop shape with few small plane structure. For the air cooling stage, it is observed that the IMC at central region shows prismatic structure whereas the peripheral region exhibits scalloped grain structure. The transition phenomenon from scalloped to prismatic structure in IMC, occurred only in soldering cooling stage. Hence, it can be concluded that the cooling stage has a strong influence on the morphology of IMC.

3.3 Numerical simulation analysis of temperature profile in micro solder joints

Under the condition of air cooling, the IMC formed a long prismatic morphology in addition to the larger plane structure. Due to the fact that the solder balls are small, it is difficult to measure the temperature distribution inside them, so the finite element method is used to simulate the temperature distribution in the solder joints. The size of the solder joint copper substrate is 2000 μm × 2000 μm × 100 μm, and the top filler metal is the hemisphere of radius 500 μm.

The steady state heat flux through the solder is given by the following heat calculation equation.

$$k_{th}\nabla^2 T = 0 \tag{7}$$

In Eq. (7), k_{th} is the thermal conductivity of Sn solder, which is taken as 31.241 W/(mK) [14]. The initial temperature of the solder-substrate medium is taken as $T_0 = 548.15$ K.

Assuming that the natural convective cooling to the air is the major heat transfer phenomenon, the boundary condition for cooling at air-solder boundary is

$$k_{th}\frac{\partial T}{\partial n} = h_{air}\left(T - T_{air}\right) \tag{8}$$

In Eq. (8), the ambient temperature T_{air} is set as 293.15 K. The convection heat transfer coefficient h_{air} is assumed as 15 W/m²K.

Finite element simulation results are shown in Fig. 4a, b. Due to the symmetry of the solder joint structure, the temperature and the temperature gradient on the center section can represent the temperature distribution of the whole solder joint. The effect of temperature distribution on the growth of IMC in the interface of 5 min is analyzed by the comparison of the temperature distribution of the air cooled IMC at 275 °C.
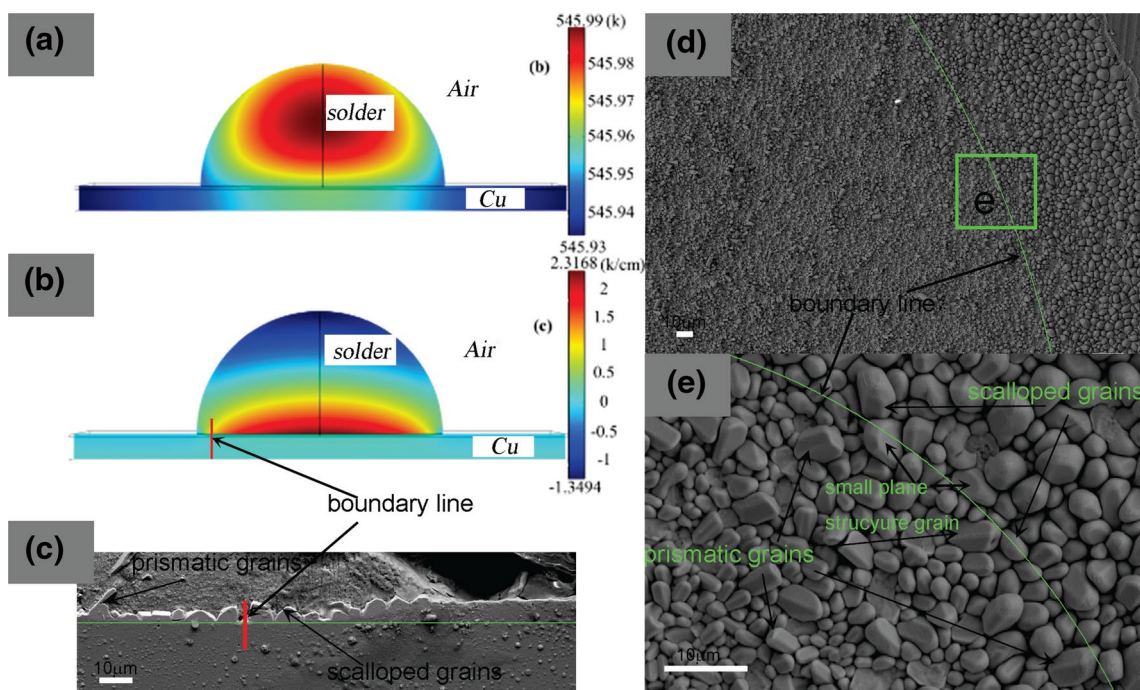
Fig. 4 Finite element method based numerical simulation results of temperature distribution (a) and temperature gradient distribution (b), and SEM image of the cross-sectional (c) and *top-view* (d–e) morphologies of IMC grains in samples treated with air cooling under 275 °C at 5 min. e is magnification of the boundary line area of (d)

As shown in Fig. 4a, the internal temperature distribution of solder joints is not uniform, the temperature inside the solder is the highest, and the interface temperature is relatively lower near the copper substrate. The internal temperature difference is not big, and the temperature difference is only 0.05 °C in the joint of the given size. The position of IMC in the joint is mainly in the interface between the solder and the copper substrate. According to the Eq. (6), internal temperature gradient are considered by the changes of W in the solder joints, as shown in Fig. 4b. The temperature gradient at the interface is maximum, and the temperature gradient at different locations of the interface is also different. The temperature gradient is the largest in the middle of the soldering interface. Moreover the temperature gradient along the vertical direction in the interface is larger than that along the horizontal plane of interface. With the temperature gradient distribution results shown in Fig. 4b, it can be interpreted that the larger the temperature gradient is, the more likely is the formation an elongated prismatic IMC. The central regions of solder ball-substrate interface in Fig. 2d, f are characterized by larger thermal gradient and thus bear prismatic IMC whereas the peripheral areas owing to smaller temperature gradient represent scalloped IMC grains. This phenomenon is also clearly observed in Fig. 4c–e. What's more, we discover that the scalloped shape and prismatic morphology of IMC has a boundary portion, so it is delimited the dividing line as the boundary line of the two kinds of IMC morphology, as marked in Fig. 4c, e, f with red and green lines. It is calculated that the distance from dividing line to the edge of solder ball is 54.9 μm. When this distance corresponding to the temperature gradient simulation diagram, we found that the temperature gradient in this region is less than the temperature gradient of the central region. That is to say, the distance from the edge to dividing line in solder joint consists with the area of the minimum temperature gradient in simulation diagram.

The simulation results of Fig. 4a, b show that the temperature gradient of the soldering interface is positive. Through Eq. (6), it is known that a small plane structure can be formed at the interface. From simulated temperature distribution and Eq. (5), the small plane forms in the region of the solder joint with larger thermal gradient. In the middle area of the solder joint, the temperature gradient is relatively large, and the space of the solder is larger, which provides more adequate supply of elements for the formation of a small plane. And on the boundary, on one hand the temperature gradient difference is small, which is not conducive to the growth of the small plane. On the other hand, the solder volume is relatively small near the boundary, resulting the growth of the small plane without adequate supplies of elements and unlikely to form elongated IMC. According to the formula (6), it

is known that in the direction of the solder, S increases with the decrease of the temperature gradient, promoting the rapid growth of IMC to the solder and forming an elongated prismatic IMC.

3.4 Growth mechanism and kinetic analysis of Cu_6Sn_5

Cu_6Sn_5 crystal structure is known to be close to hexagonal close-packed [15] and the miller indices of crystallographic plane index of the small plane is $(10\bar{1}0)$ [16]. It is known that $(10\bar{1}0)$ has the largest inter-planer spacing in the indices of crystallographic plane. According to the law of Bravais, crystal plane performed by the crystal morphology has relation with inter-planer spacing. Crystal plane with larger inter-planer spacing has less attraction to the foreign atom. The crystal plane growth rate will be very small, so crystal plane with large inter-planer spacing will be left. In context of small plane growth explained through 2D nucleation growth mechanism; more vacancies exist in the spreading surface of small plane which makes the side face of the plane to grow in the mode of continuous growth mechanism, such as shown in Fig. 5a of the small plane growth principle diagram. Crystal interface free energy (Z) can be expressed as following [17]

$$Z = \gamma A \qquad (9)$$

Among them, A is the crystal surface area, and γ is the surface energy of the crystal in unit area, which is equal to the surface tension numerically. As shown in Fig. 5a,
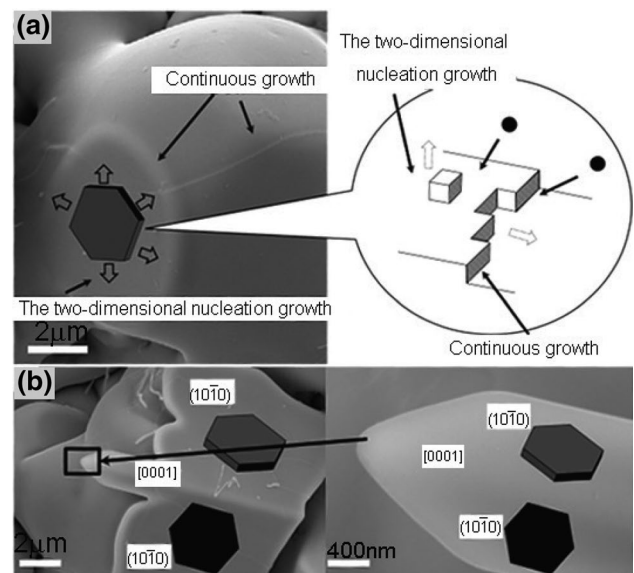
Fig. 5 Schematic diagram of the growth mechanism of faceted microstructure (**a**) and microstructure images of Cu_6Sn_5 grains (**b**)

the top of the crystal surface has only one plane providing nucleation and growth of atomic, while the side consists at least two surfaces. According to Eq. (9), the side of the small plane has a larger space for atomic growth. With a greater free energy, it can easily attract atomic to the growth position. Therefore, the growth rate of Cu_6Sn_5 in the vertical direction of small plane is much smaller than the growth along the small plane.

Considering the view of crystallography, the straight line that is parallel to $(10\bar{1}0)$ of two crystal planes index is the crystal zone axis of the two crystal planes. The axial plane $(10\bar{1}0)$ index is [0001]. Although some scholars [15, 16] have used experimental methods to measure the crystal face $(10\bar{1}0)$ with preferring orientation as [0001], its close relationship with prismatic IMC formation has not been taken into account till now. As shown in Fig. 5, two small planes growing to a certain size will touch with each other. When there is an angle difference between the two planes, the crystal surface on the crystal zone axis cannot pass through each other due to the mutual inhibition. Therefore, the crystal surface at the junction can only grow along the crystal zone axis with outward direction. Cu_6Sn_5 in [0001] crystal exists along the spiral axis [15], enabling it to grow rapidly in the direction. When crystal zone axis is towards the solder, element supply in this direction is sufficient, promoting the Cu_6Sn_5 to form elongated prismatic morphology. When the crystal zone axis is parallel to the interface, elements supply along the interface is less than the perpendicular direction, so it can not form a slender prismatic morphology. In other position of small plane, there was an appearance of the curvature of the semicircle due to the isotropic growth as shown in Fig. 5. Therefore, in the junction of two crystal planes, there is the formation slender junction morphology. In Fig. 5, for the amplified portion of the top of the prism, it could be observed that the top of prism as well as the other position of small planes is semi circle with curvature. Combining Eq. (5) with the results of numerical simulations shown in Fig. 4, it is inferred that the rough interface should be in relatively high temperature, which confirms the side is the rough interface controlled by continuous growth mechanism.

In the process of cooling stage, the saturated concentration of copper in the solder decreases with the decrease of temperature, which makes large amounts of copper precipitate from solder. Qu et al. [10] have highlighted that soldering interface IMC growth mechanism is a dynamic process constituting of simultaneous precipitation and dissolution. In the cooling stage, reduction in the copper saturated concentration of the liquid filler inhibits the dissolution of IMC, and the precipitation of copper will be on the surface of IMC. Thus, this leads the existing IMC to undergo accelerated heterogeneous nucleation growth. Cu continues to precipitate and

grow as IMC after interfacial reaction with Sn, thereby prompting the IMC have small plane morphology. This can cause the two-dimensional nucleation and continual growth of prismatic IMC.

From the dynamic point of view, the temperature reduction will cause the flux change that can subsequently alter the formation rate of IMC in the cooling stage, such as shown in Fig. 6. In the cooling phase, the activity of copper decreases with the decrease of temperature, which causes the reduction in diffusion flux of copper towards solder (i) through channels of IMC grains (J_{solder}) and (ii) from IMC surface (J_{IMC}). At the same time, with lower saturated copper concentration in the solder (C_0) at decreasing temperature, there is the precipitation of Cu back to the IMC from solder in the form of $J_{solder/IMC}$, flux. The grain boundary between IMC is gradually clogged with the effect of $J_{solder/IMC}$ thus leading to the retardation in Cu transport via J_{solder}. At the same time, precipitated copper solder also inhibits the dissolution of IMC via the flux $J_{IMC/solder}$. This would eventually proceed to the subsequent formation of scallop and small plane IMC growth. With the formation IMC small plane, the curvature of the surface is changed, which results the change in concentration distribution along the surface of IMC. Moreover, the annexation between adjacent IMCs is inhibited. A small plane is first formed in the lower position of Cu_6Sn_5, and it has rapid growth only toward to the liquid solder on the hemispherical surface due to the constraint of growth space.

In the analysis, the growth behavior of interface IMC in cooling stage is affected by copper precipitation in the solder and degree of supercooling. The precipitation of copper in the solder provides the necessary elements for the rapid growth of IMC in the cooling stage, while the degree of supercooling provides the driving force for IMC morphology transition during the cooling phase.
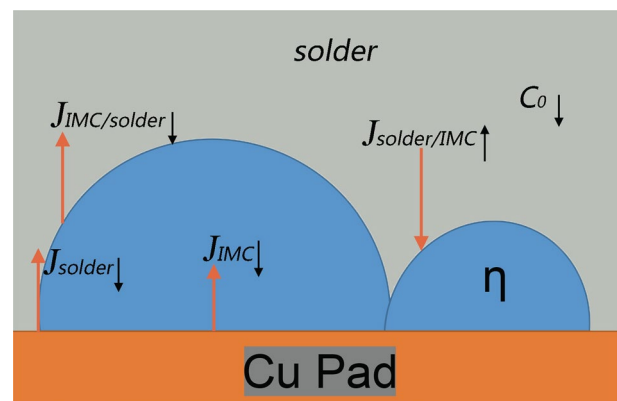
Fig. 6 Schematic diagram of growth flux variation of the interfacial IMC in cooling stage
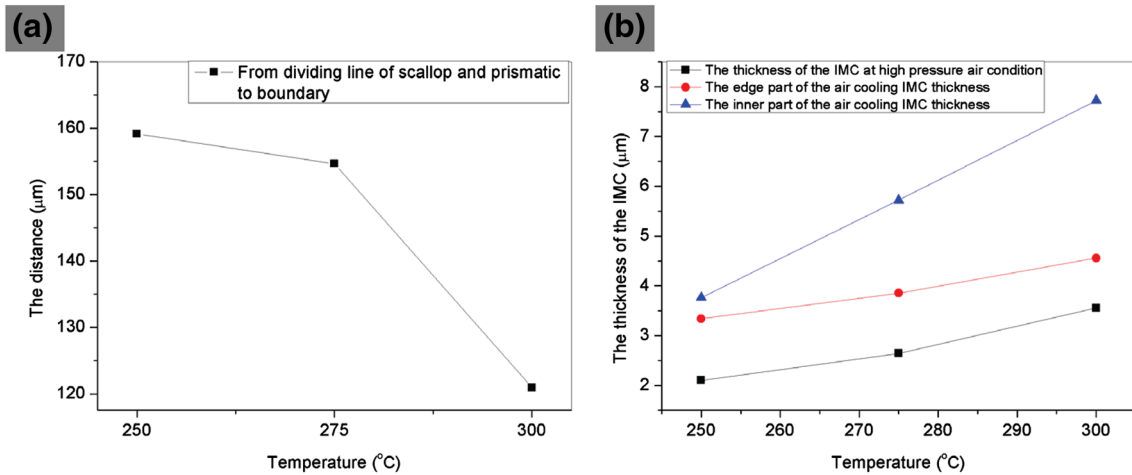
Fig. 7 Distribution diagram of dividing line from inner to boundary of solder joint in air cooling (**a**) and the thickness of IMC layer by air cooling and high-pressure air (**b**)

3.5 Influence of temperature on the morphology, regional distribution and thickness of IMC

The radial length between the solder exterior and the demarcation circumference separating the scalloped IMC from prismatic IMC has been plotted in Fig. 7a for three soldering temperatures. In the similar way, the curves of Fig. 7b represent the average IMC thickness at two different spatial locations of solders with different temperatures (250/275/300 °C). The thickness data correspond to reaction of liquid solders with the polycrystalline Cu substrate during the time period of 5 min of air cooling. Additionally, the thickness of IMC for experiment corresponding to application of high pressure air has been included in the figure.

With the rise in soldering temperature, the demarcation line between prismatic and scallop morphology of IMC continues to shift towards the edge of solder joint as illustrated in Fig. 7a. Moreover, with the increasing soldering temperature, the thickness of IMC layer increases. As shown in Fig. 7b, the thickness of IMC corresponding to air cooling is larger than the value corresponding to experiment with high pressure air. In the air cooling experiment based measurements, the inner side IMC is observed to be thicker than the IMC at the edge location. With the rise of soldering temperature, the area ratio of scallop-like morphology IMC to the prismatic shape in the solder joint is reduced from 0.2178 to 0.1680, that is to say, the dividing line between the prismatic shape and the scallop-like shape constantly extends to the edge of solder joint. At the same time, the thickness of the IMC in the inner region of the spherical solder joint reaches to 7.7245 µm, while the thickness of the IMC at the edge only reaches to 4.556 µm.

The solubility of Cu atoms in the liquid solder decline with the soldering temperature decreasing. Then the Cu atoms precipitate in the form of compounds during cooling stage. In order to reduce the nucleation free energy, the newly generated Cu_6Sn_5 that are obtained as a result of precipitation of Cu from supersaturated Sn solder during cooling, tend to form small planar structure on the surface of existing scallop Cu_6Sn_5. As known by Eq. (6), it is easy to form small plane in a high degree of cooling place, and the formation of small plane makes liquid solder appeared Cu-rich zone at perpendicular directions of small plane. Those region will be precipitated first, and further promote Cu_6Sn_5 to grow along small plane extending to liquid solder. Finally Cu_6Sn_5 acquires prismatic morphology. Those grains grow in vertical interface have gaps, retaining the desired channel for reaction which has more superiority in growth. So, it can continue to grow rapidly in the direction perpendicular to the interface, and grow into prismatic Cu_6Sn_5. As a result, the area of scallop morphology reduces, while the area of the plane and prismatic morphology increases. The IMC morphology partition line constantly goes to the edge.

The rise of soldering temperature causes an increase in the dissolution of Cu, and the dissolution of Cu can be expressed in the consumption of the thickness of Cu substrate indirectly, according to dynamics equations (10) of the consumption of Cu and the time, temperature in eutectic Sn–Pb solder [2]:

$$\Delta h = A \exp\left(\frac{-Q}{kT}\right) t^n \tag{10}$$

where Δh is the consumption of the thickness of Cu substrate, Q is the activation energy, k is the Boltzmann constant, T is temperature, t is the reaction time, and A and

n are the parameters. The activation energy and various parameters are stable when the reaction temperature is certain and available in a certain way; here we assume them as a fixed value. As can be seen from the Eq. (10), consumption of Cu substrate expressed in terms of dissolved thickness is in proportion to the reaction temperature. So with the rise of the soldering temperature, the consumption of Cu substrate or dissolution of Cu into solder increases, resulting in the enrichment of Cu element in the solder. At the same time the corresponding temperature gradient increases, giving rise to the extension of cooling time and the decrease of cooling rate. This will subsequently cause greater precipitation and deposition of Cu in a wider geometric area of interface during cooling to cause more pronounced growth of Cu_6Sn_5 and extension of the prismatic morphology towards the edge. With greater degree of supercooling and lower quantity of solder at the edge of the joints, the thickness of IMC layer in this part of solder joint is bigger than the inner portion. However, because of high-pressure air removing excess liquid solder, the IMC does not have the chance for secondary growth. Therefore, the thickness of IMC layer is minimum among the three conditions.

4 Conclusions

In this study, Cu_6Sn_5 morphological evolution mechanism and kinetic analysis of the cooling phase spherical joints on the Sn/Cu solder liquid–solid interface was investigated. The results are summarized as follows:

1. The formula derived from the crystal growth theory shows that the temperature gradient in the liquid/solid interface (W) of spherical solder joint determines the morphology of the IMC in the cooling stage. When W is positive, the value of S is positive, forming a small plane; but when W is negative, the value of S is negative, not forming a small plane.
2. The morphology of IMC using high pressure air to remove excess liquid filler metal (heat preservation stage) is scallop-like with small plane. However, the cooling stage during soldering has a great influence on the morphology evolution of IMC in spherical solder joints. Partition phenomenon is exhibited by the morphology of IMC for spherical solder joints, with the edge portion representing scalloped pattern with small plane whereas the central portion are characterized by prismatic shapes.
3. Internal temperature field distribution in lead-free solder joint as simulated by finite element shows that temperature gradient at the center core of the sample is significantly greater than that in the edge. Moreover, owing to this distribution of temperature field, the central region has a tendency to form a small planar structure, grows into prismatic morphology of IMC, eventually leading to partition phenomenon in IMC morphology (prismatic shape in center whereas scalloped shape in edge) during the cooling stage.
4. With the rise of soldering temperature, the area ratio of scallop-like morphology IMC to the prismatic shape in the solder joint is reduced from 0.2178 to 0.1680, that is to say, the dividing line between the prismatic shape and the scallop-like shape constantly extends to the edge of solder joint. At the same time, the thickness of the IMC in the central region of the spherical solder joint reaches to 7.7245 μm, while the thickness of the IMC at the edge only reaches to 4.556 μm.

References

1. E. Wood, K. Nimmo, J. Electron. Mater. **8**, 709–713 (1994)
2. H.M. Kim, K.N. Tu, Phys. Rev. B **53**, 16027–16034 (1996)
3. Y.G. Lee, J.G. Duh, J. Mater. Sci. **33**, 5569–5572 (1998)
4. K.H. Prakash, T. Sritharan, Acta Mater. **49**, 2481–2489 (2001)
5. H. Ardebili, M. Pecht, *Electronic Packaging Technology and Reliability* (Chemical Industry Press, Beijing, 2012), pp. 5–8
6. D.K. Shangguan, *Lead-free Solder Interconnects and Reliability* (Publishing House of Electronics Industry, Beijing, 2008), pp. 60–66
7. M. Yang, M.M. Li, L. Wang, Y. Fu, J. Kim, J. Electron. Mater. **40**, 176–188 (2001)
8. H.T. Lee, H.M. Chen, H.M. Jao, T.L. Liao, Mater. Sci. Eng. **A358**, 134–141 (2003)
9. H.T. Ma, L. Qu, M.L. Huang, L.Y. Gu, N. Zhao, L. Wang, J. Alloys Compd. **537**, 286–290 (2012)
10. L. Qu, N. Zhao, H.J. Zhao, M.L. Huang, H.T. Ma, Scr. Mater. **72–73**, 43–46 (2014)
11. N. Yan, *Physical Basis of Crystal Growth* (Shanghai Science and Technology, Shanghai, 1982), pp. 189–451
12. K. Zhang, L. Zhang, *Crystal Growth of Science and Technology* (Science Press, Beijing, 1997), p. 39
13. G. Hu, *Material Science Basis* (Profile of Shanghai Jiao Tong University Press, Shanghai, 2001), pp. 199–224
14. M.V. Peralta-Martinez, W.A. Wakeham, Thermal conductivity of liquid tin and indium. Int. J. Thermophys. **22**, 395–403 (2001)
15. A. Gangulee, G.C. Das, M.B. Bever, Metall. Trans. **4**, 2063–2066 (1973)
16. M. Yang, Y. Cao, S.M. Joo, H.T. Chen, X. Ma, M.Y. Li, J. Alloys Compd. **582**, 688–695 (2014)
17. X.Y. Liu, M.L. Huang, Y.H. Zhao, C.M.L. Wu, L. Wang, J. Alloys Compd. **492**, 433–438 (2010)